

## A COAXIAL MAGIC-T\*

T. Morita and L. S. Sheingold<sup>†</sup>  
Cruft Laboratory, Harvard University  
Cambridge, Massachusetts

### Abstract

A coaxial hybrid junction is described whose performance is analogous to a waveguide magic-T. The design of three different types of coaxial magic-T is discussed. Standing-wave characteristics of an experimental model of each type are given. Experimental results indicate that standing-wave ratios less than 2 looking into any arm can be obtained easily over a frequency band of about 10 per cent. Owing to the structural symmetry of the device, the decoupling between shunt and series arm is of the order of 40 db.

An application of the coaxial magic-T to phase measurements is described. This method of phase measurement is independent of the amplitude of the unknown signal.

### Principle of Operation

#### Type I

Figure 1 is a schematic diagram of the coaxial hybrid junction. This consists essentially of a coaxial-T junction with a shielded loop the axis of which is located at the center of the "T". The terminals of the coaxial hybrid junction are numbered to correspond to the usual convention. Owing to the symmetry of the structure, a voltage applied to the shunt arm (3) will appear equal in phase and magnitude at terminals (1) and (2). Since the current divides into equal and oppositely directed currents at the junction of the "T", the total magnetic flux threading the loop is zero. Hence, there is no coupling between terminals (4) and (3). By reciprocity there is no coupling between terminals (3) and (4) when voltage is applied at terminals (4) and equal loads are placed at terminals (1) and (2). When the series arm (4) is excited, because of the odd-symmetry nature of the loop, fields are excited in arms (1) and (2) which have odd-symmetry and hence equal but oppositely phased voltages are applied across terminals (2) and (1). Thus, if both arms (4) and (3) are excited simultaneously, the vector sum of the two voltages appear across arm (2) while the vector difference appears across arm (1). This is identical to the operation of the hybrid coil or the waveguide magic-T.

\* The research reported in this document was made possible through support extended Cruft Laboratory, Harvard University, jointly by the Navy Department (Office of Naval Research), the Signal Corps of the U. S. Army, and the U. S. Air Force, under ONR Contract N5ori-76, T. O. 1.

† L. S. Sheingold is now with the Boston Engineering Laboratory of Sylvania Electric Products Inc., Boston, Massachusetts.

The amount of coupling from arm (4) may be controlled by either varying the spacing of the loop to the horizontal center conductor of the coaxial-T or by increasing the area of the loop. Since the coupling can be shown to vary logarithmically with the spacing, while only linearly with the area, it is essential for the spacing to be small to insure close coupling of the loop to arms (1) and (2). A shielded loop is used to make the loop symmetrical about the junction and to eliminate the dipole mode.<sup>1</sup> A short-circuiting plunger has been incorporated to make the loop arm tunable over a wider frequency range. In general the dimension of the loop should be about a half-wavelength and the short-circuiting plunger placed a half-wavelength away from the gap terminals. In Figure 2 is shown a photograph of an experimental model with a design wavelength of 9.91 cm.

### Type II

Since the construction of a small shielded loop is not practical for mass production, an alternative design using the same principle is shown in Figure 3. Here the shielded loop has now been replaced by a straight coaxial line with a small gap in the outer conductor.

### Type III

In the description of the types I and II coaxial hybrid junctions presented above, the coupling between the series arm (4) to the loads at terminals (1) and (2) is analogous to the coupling between two coils of a low-frequency transformer. In order to obtain a broad-band matched condition looking into the series arm (4), it is desired to obtain tight coupling between the loop and the loads. Since it is theoretically difficult to obtain the proper spacing required, a second variation of this coaxial magic-T, which employs direct coupling, has been designed. This is similar to the one considered by Pound.<sup>2</sup> Since the coupling is unity, the impedance behavior of this structure is more readily analyzed. The sketch and photograph of the experimental model are shown in Figure 4.

## Experimental Results

### Type I

Figure 5 is a plot of the input standing-wave ratio for the shunt and series arm. The short-circuiting plunger in the series arm has been adjusted for optimum bandwidth. No attempt was made to match the shunt arm. The behavior of the series arm is identical to the behavior of an over-coupled transformer with the impedance curve making a loop over the  $r = 1, x = 0$  point on the Smith chart, so that two minimum standing-wave ratios are obtained. For wider spacing of the loop arm, only a single minimum is obtained corresponding to a loosely coupled transformer.

A similar coaxial magic-T was scaled down to operate at a center wavelength of 5.5 cm. This was designed for operation as a balanced mixer with the local oscillator feeding into the series arm. In order to pad the local oscillator and to increase the bandwidth of the series arm, a lossy dielectric was placed in the coaxial line forming the loops. A bandwidth ( $VSWR \leq 2$ ) of 13 per cent as compared to 6.6 per cent in the 9.91-cm. model was obtained for the series arm.

## Type II

Figure 6 is the operating characteristic of the type II coupler at a center-wavelength of 12 cm. A matching section has been incorporated into the shunt arm. The bandwidth obtained here is of the order of 10 per cent.

## Type III

The analysis of the magic-T is facilitated by the use of the scattering matrix. Since the structure is lossless, symmetrical, and all terminals have the same characteristic impedance, the scattering matrix is unitary and is written as:

$$\|S\| = \begin{vmatrix} S_{11} & 0 & S_{13} & S_{14} \\ 0 & S_{22} & S_{13} & S_{14} \\ S_{13} & S_{13} & S_{33} & 0 \\ S_{14} & S_{14} & 0 & S_{44} \end{vmatrix}$$

where  $S_{mm}$  is the reflected wave at terminal  $m$  due to a unit wave incident on the junction at terminal  $m$ , and  $S_{mn}$  is the transmitted wave at terminal  $n$  due to a unit wave incident at terminal  $m$ . The fact that  $S_{34} = S_{43} = 0$  is verified experimentally by placing a short-circuiting plunger on terminal (3) and measuring the impedance looking into arm (4) as a function of the position of the short-circuiting plunger. If  $S_{34} = S_{43} = 0$ , as the position of the short circuit is varied, the impedance looking into arm (4) will not change. A similar procedure can be applied to show that  $S_{12} = S_{21} = 0$ .

Since the matrix is unitary, the sum of the squares of the absolute magnitudes of any row or column is unity. Hence from the third and fourth columns one obtains

$$|S_{13}|^2 = \frac{1 - |S_{33}|^2}{2} \quad \text{and} \quad |S_{14}|^2 = \frac{1 - |S_{44}|^2}{2}$$

Thus it is apparent that if one can show experimentally that  $S_{34} = S_{43} = 0$ , then only measurements of the reflection coefficient looking into the shunt and series arm are required to obtain the absolute values of the elements of the scattering matrix.

Figure 7 is the plot of the squares of the elements of the scattering matrix for the type III junction. In order that the voltage standing-wave ratio be less than 2, the square of the diagonal elements should be less than 0.111, while  $|S_{13}|^2$  and  $|S_{14}|^2$  should be between 0.445 and 0.500. The short-circuiting plunger in arm (4) has been fixed for best match at the center wavelength of 8.94 cm. A bandwidth of 9.2 per cent is obtained.

Figure 8 is a plot of the input standing-wave ratio behavior of the series arm for a fixed frequency as the position of the short-circuiting plunger is varied. These curves exhibit the same behavior as those of the types I and II junctions.

In Figure 9 is shown the input standing-wave ratio for the series and shunt arms as the wavelength is varied from 8 to 11 cm. The position of the short circuit in the series arm has been adjusted to obtain a minimum SWR for each frequency. The results show that the position varies linearly with the wavelength, so that this property should be useful for balanced mixer operation in tunable receivers where the plunger can be tracked with the tuning of the local oscillator cavity. Since no attempt was made beyond the initial design consideration, it is believed that with standard broad-banding procedure a better match can be obtained, especially in the shunt arm.

The measurement of decoupling between the shunt and series arm is very sensitive to the balance of the loads. The VSWR of the loads used varied from 1.1 to 1.2 over the range of measurement.

### Typical Applications

There are numerous practical applications of the coaxial magic-T. It can be used to obtain a suppressed carrier system or a single side-band system. Its use as a bridge or as a balanced mixer in receivers is well known.<sup>3</sup>

One of the applications for which the magic-T has proved useful is in the measurement of phase. Phase measurement procedure used in the frequency range under consideration has normally involved the addition of a reference signal and the signal whose phase is to be measured. The reference signal is adjusted until it is 180 degrees out of phase with the unknown signal, so that a null is obtained. This procedure is reliable only when the amplitude of the reference signal is of the same order of magnitude as the unknown signal. The method to be described is primarily independent of the signal amplitude and is similar to the homodyne system of phase measurement.

Figure 10 is the block diagram of the balanced detector method of phase measurement. A radio-frequency signal (either modulated or unmodulated) of variable phase is injected into the series arm (4) while the signal under test is fed into the shunt arm (13). The vector sum of the signals from arms (3) and (4) is impressed across the crystal load of terminal (2) while the vector difference is applied across the crystal load at terminal (1). A receiver which takes the differences of the detected voltage across crystals (1) and (2) is connected as shown in Figure 11. When the reference signal is adjusted to be 90 degrees out of phase with the signal under test, a sharp null is obtained. As may be seen, the null always goes into noise and at the 90-degree point the meter output has a cusp rather than a zero slope for the former method. A phase ambiguity of 180 degrees exists; however, for most applications this is not serious.

### Acknowledgement

The authors wish to thank Mr. Edgar W. Matthews, Jr. and Mr. Robert Blanchard of Trans-Sonics Inc. for the use of the data obtained on the Type II Coaxial Magic-T.

### References

1. D.D. King, Measurements at Centimeter Wavelength, D. Van Nostrand, New York, 1952, pp. 275-277.
2. R.V. Pound, Microwave Mixers, McGraw-Hill, New York, 1948, p. 268.
3. D.D. King, op. cit., pp. 226-233.

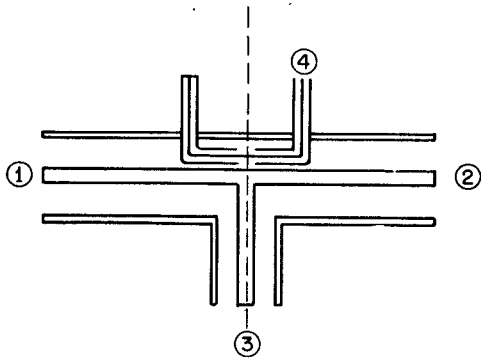


Fig. 1 - Coaxial hybrid junction:  
Type I.

Fig. 2 - Experimental model of  
coaxial hybrid junction:  
Type I. →

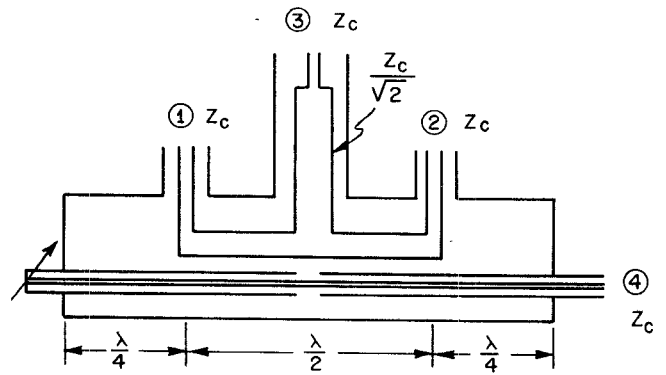
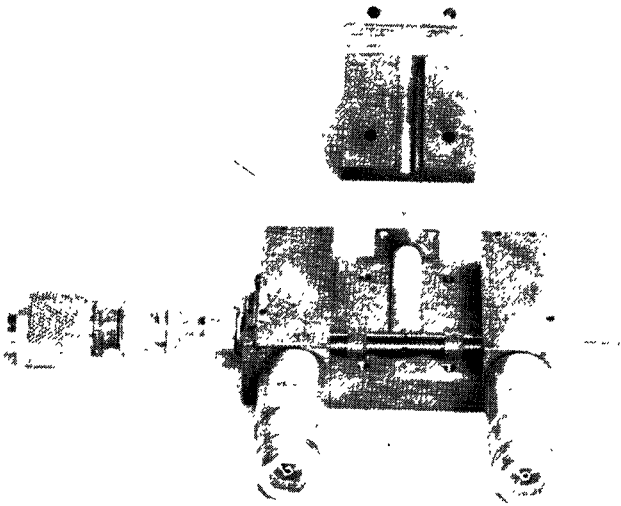
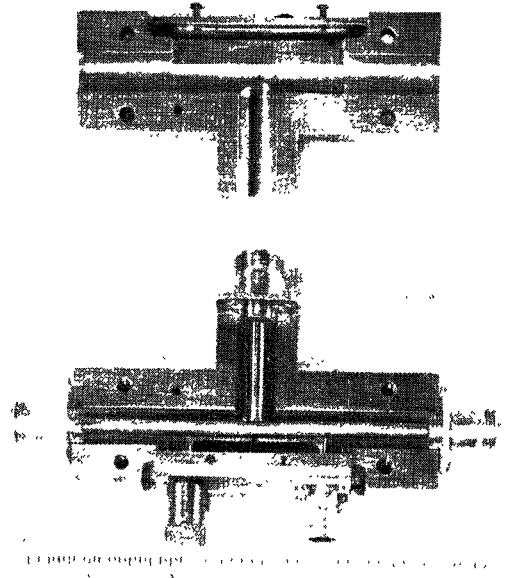


Fig. 3 - Coaxial hybrid junction:  
Type II.

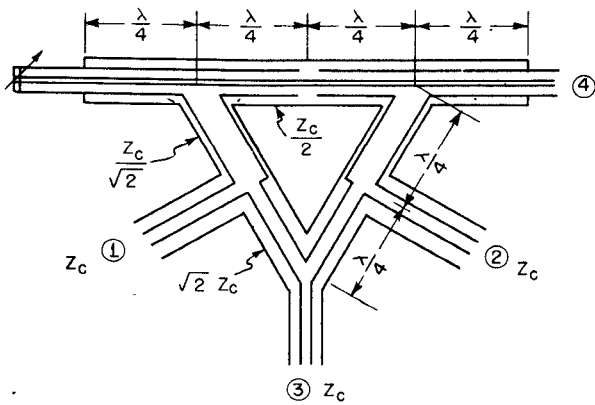


Fig. 4 - Coaxial hybrid junction:  
Type III.

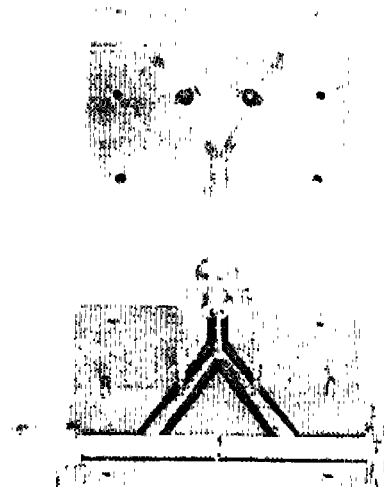
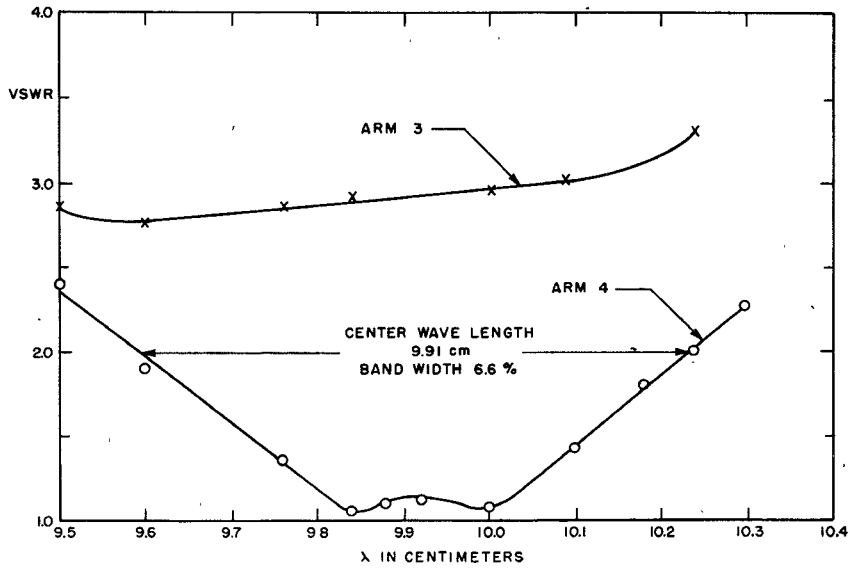
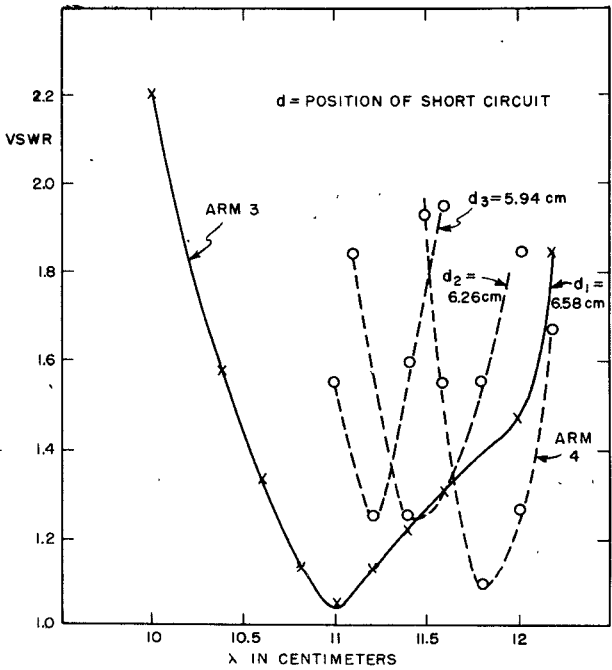


Fig. 5

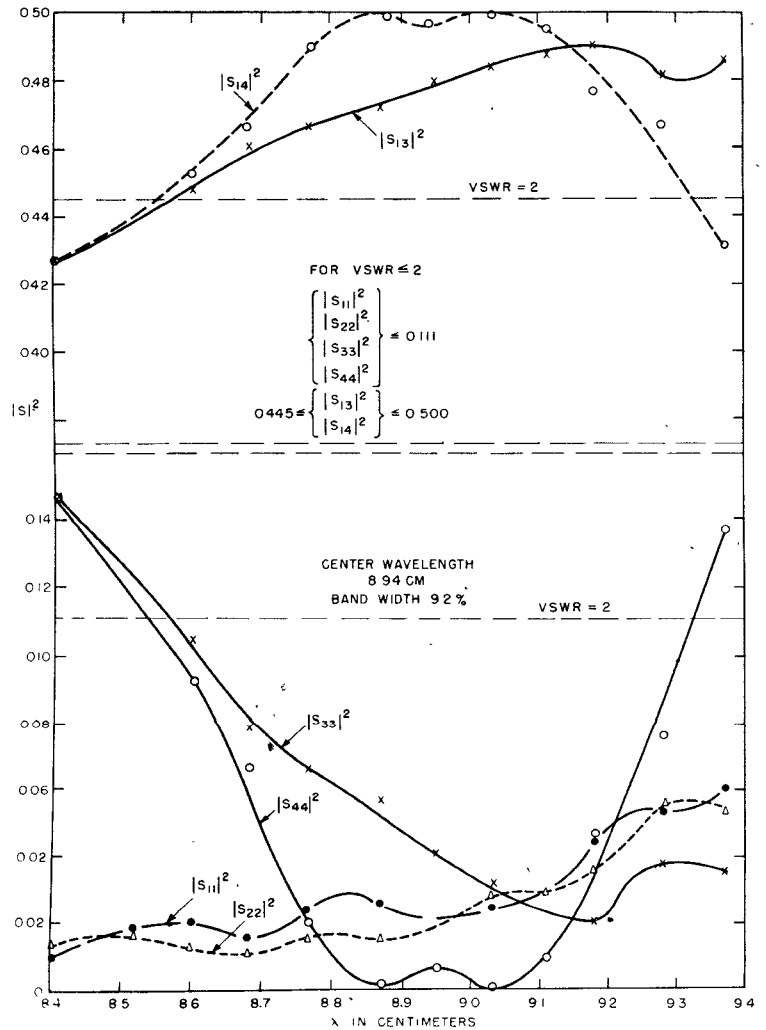


VOLTAGE STANDING-WAVE RATIO CHARACTERISTICS OF COAXIAL HYBRID JUNCTION. (TYPE I)



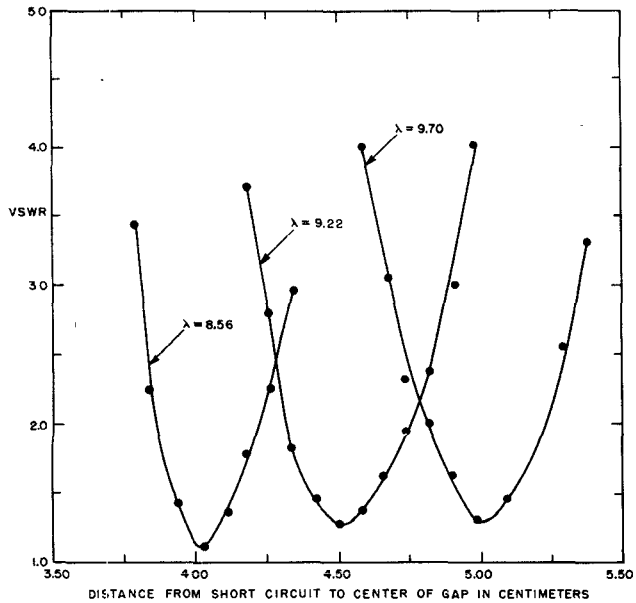
VOLTAGE STANDING-WAVE RATIO CHARACTERISTICS OF COAXIAL MAGIC T (TYPE II)

Fig. 6



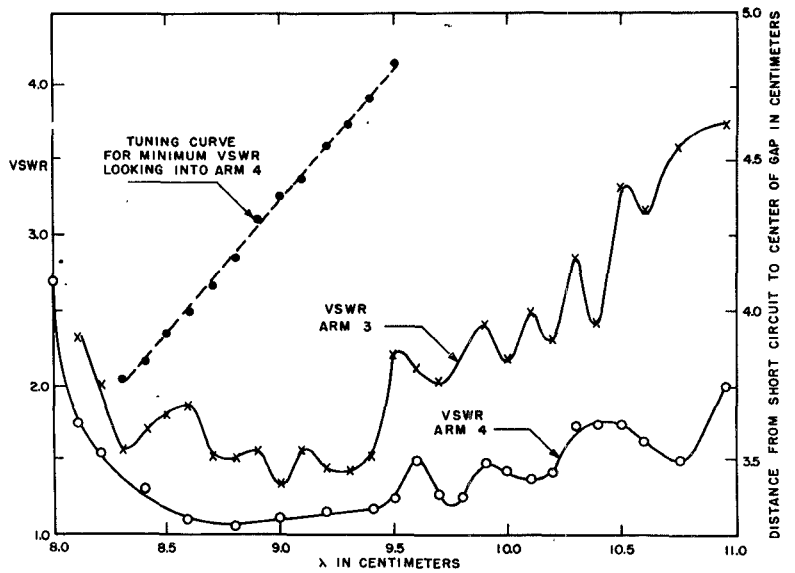
SCATTERING MATRIX ELEMENTS FOR TYPE III

Fig. 7



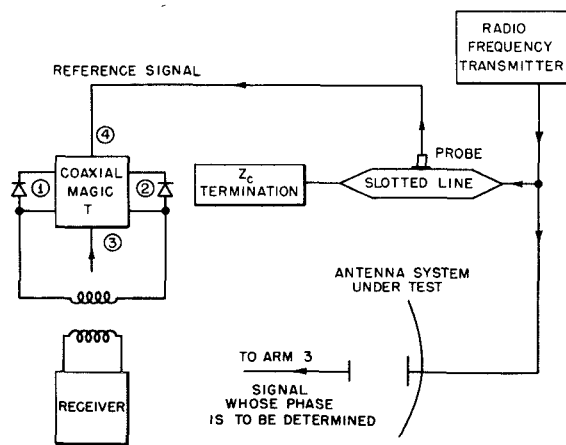
VOLTAGE STANDING WAVE RATIO OF ARM 4 AS A FUNCTION OF POSITION OF SHORTING PLUNGER. (TYPE III)

Fig. 8



INPUT VOLTAGE STANDING-WAVE RATIO OF ARMS 3 AND 4 WITH SHORT CIRCUIT ADJUSTED FOR MINIMUM VSWR (TYPE III)

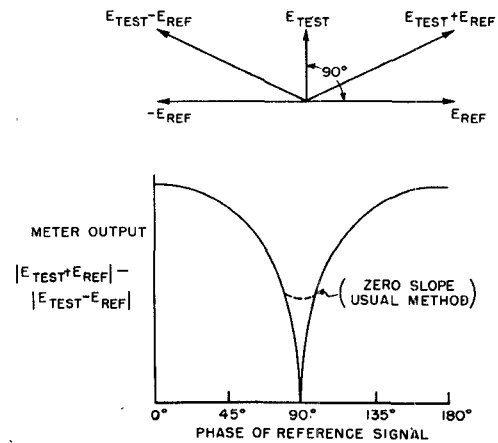
Fig. 9



BLOCK DIAGRAM OF EQUIPMENT

BALANCED DETECTOR METHOD OF PHASE MEASUREMENT

Fig. 10



VECTOR DIAGRAM OF PHASE RELATIONS

Fig. 11